

Homoleptic carbene complexes[☆]

Part VIII. Hexacarbene complexes

Robert Fränkel^a, Ulrich Kernbach^b, Maria Bakola-Christianopoulou^c, Ulrike Plaia^d,
Max Suter^{a,1}, Werner Ponikwar^{a,1}, Heinrich Nöth^{a,1}, Claude Moinet^e,
Wolf Peter Fehlhammer^{b,*}

^a Department Chemie der Ludwig-Maximilians-Universität München, Butenandtstraße 5-13 (Haus D), D-81377 Munich, Germany

^b Deutsches Museum, Museumsinsel 1, D-80538 Munich, Germany

^c Department of Chemical Engineering, Aristotele University, GR-540 06 Thessaloniki, Greece

^d Institut für Anorganische und Analytische Chemie der Freien Universität Berlin, Fabeckstraße 34-36, D-14195 Berlin, Germany

^e Laboratoire d'Electrochimie et Organoméalliques, UMR CNRS 6509, Université de Rennes 1, Campus de Beaulieu,
F-35042 Rennes Cedex, France

Received 10 August 2000; accepted 25 September 2000

Abstract

A modified in situ preparation of the chelating monoanionic tricarbene ligands hydrotris(3-alkyl-imidazoline-2-ylidene-1-yl)borate (TRIS^R, R = Me, Et) is reported along with the syntheses of the hexacarbene iron(III) [Fe(TRIS^R)₂](BF₄) (R = Me (**3a**), Et (**3b**)) and cobalt(III) complexes [Co(TRIS^R)₂](BF₄) (R = Me (**4a**), Et (**4b**)) and the usual spectroscopic data (IR, ¹H-, ¹³C- and ¹¹B-NMR, MS (pos-FAB)). The X-ray structure determinations of **3b** and **4b** reveal their spherical quasi-C₆-cage structures of approximate S₆ geometry and the absence of any metal to carbon multiple bonding as expected for the combination of high valent metals with electron-rich, doubly heteroatom-stabilized carbenes. In addition, electrochemical studies have been undertaken in order to understand the spontaneous formation of the hexacarbeneiron(III) species **3** from iron(II) starting materials and TRIS^R. CV and CPC measurements show that both, the reduced Fe(II)- and the oxidized Fe(IV)-complex are accessible and stable, i.e. no chemical decomposition follows the electrochemical reduction and oxidation processes. However, Fe(TRIS^R)₂ appears very sensitive towards any oxidation means. A second approach to hexacarbene metal complexes, viz. that via functional isocyanides — the 2-hydroxyalkylisocyanides CN-CH₂CH₂-OH and CN-CH₂CHMe-OH — is described in summary: these isocyanides which can be regarded as 'masked cyclic N,O-carbenes' isomerize (cyclize) in the presence of higher valent metals such as Co(III), Rh(III) and probably also Pt(IV) and Cr(III) to give the complexes [M(CN(H)CH₂CHRO)₆]Cl₃·5H₂O (M = Co, R = H (**5a**), Me (**5b**); M = Rh, R = H (**9a**), Me (**9b**)), [M(CN(H)CH₂CHRO)₆](PF₆)₃ (M = Co, R = H (**6a**), Me (**6b**); M = Rh, R = H (**10a**), Me (**10b**)), [Co(CN(H)CH₂CHRO)₆](BPh₄)₂ (R = H (**7a**), Me (**7b**)), [Pt(CN(H)CH₂CHRO)₆](PF₆)₄ (R = H (**11a**), Me (**11b**)) and [Cr(CN(H)CH₂CHRO)₆](PF₆)₃ (R = H (**12a**), Me (**12b**)). The X-ray structure determination of **5a** shows a highly symmetric carbene species (3 bar) co-existing in the crystal with lattice water and chloride anions all of which are involved in a complex three-dimensional network of hydrogen bonds. © 2001 Elsevier Science B.V. All rights reserved.

Keywords: Tricarbene chelating ligands; Homoleptic carbene complexes; X-ray structures

1. Introduction

The number of transition metal carbene complexes is legion today [1], yet only a handful is homoleptic consisting almost exclusively of linear dicarbene-gold and square planar tetracarbenenickel to platinum complexes. In 1985, however, we had reported on the first hexacarbene complexes which were obtained with

[☆] For Part VII, see Ref. [5].

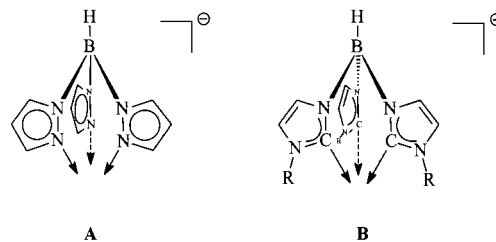
* Corresponding author. Tel.: +49-89-2179313; fax: +49-89-2179425.

E-mail address: wpf@extern.lrz-muenchen.de (W.P. Fehlhammer).

¹ X-ray structure determinations.

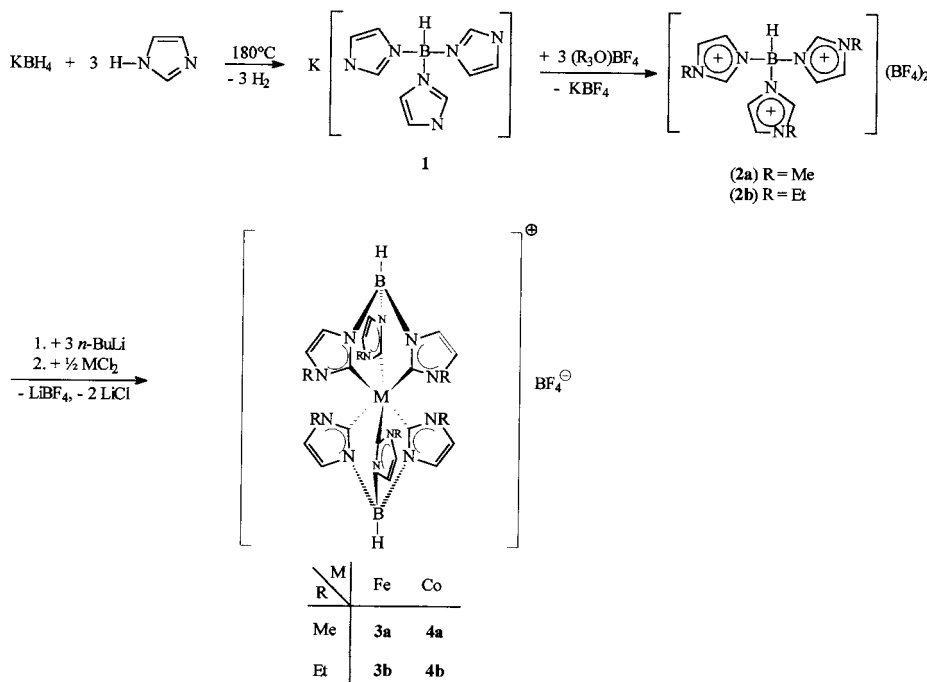
Co(III) and Rh(III) as the central metals [2]. The procedure chosen was that of reacting higher valent metal compounds with ‘functional’ isocyanides of the kind CN–CHRCHR’–OH which readily undergo intraligand cyclization with formation of oxazolidin-2-ylidene metal species. The synthetic principle had been studied thoroughly with divalent metal compounds of the nickel triad [3] and extended to cobalt and rhodium applying for the first time quasi-nonorganometallic conditions, i.e. protic media through which air was passed to maintain a metal oxidation state of III. Additional data on this type of compounds including a new and more precise X-ray structure analysis of a hexakis(oxazolidin-2-ylidene)-cobalt species are presented in this paper.

This very efficient synthetic procedure for poly- and percarbene species has been complemented recently by the in situ-preparation of the triscarbene tris(imidazolin-2-ylidene)borate (TRIS^R (B)) which is the C-isomer of Trofimenko’s well-known tris(pyrazolyl)borate (A), a perfect chelating ligand for the construction of tris- and hexa-N-coordinated metal complexes [4]. With TRIS^R, bischelated hexacarbene complexes can be obtained practically as easily as the N-analogues; three new hexacarbene iron(III) and cobalt(III) complexes are described in the following in addition to the methyl derivative of the iron(III) species reported earlier [5].



2. Syntheses of bischelated hexacarbene complexes of Fe(III) and Co(III) by the free carbene route

The tricarbene ligand TRIS^R (B) is synthesized in three steps as described in principle in an earlier paper [5]. Modifications have been made particularly in step 1 where we abandoned the procedure of Zaidi et al. because of the unsatisfactory yield and purity of the product [6]. Tris(imidazolyl)borate (1) is now synthesized by fusing together of imidazole and borate in analogy to Trofimenko’s preparation of potassium poly(1-pyrazolyl)borates [7]. In a second step, 1 is then trisalkylated with the respective methyl or ethyl oxonium salt to give the dicationic tris(imidazolium)borate salts 2a and 2b. On the latter, an X-ray structure analysis has been carried out [8]. Deprotonation of 2 is achieved with three equivalents of butyllithium, and the in situ produced monoanionic tricarbene is directly reacted with the metal chloride



Scheme 1. Preparation of the bischelated hexacarbene complexes 3 and 4.

Table 1
Selected IR data for compounds **1–12**(cm⁻¹) (KBr)

Complex	$\nu(\text{CH})$	$\nu(\text{BH})$	Others ^a
1	3137s, 3123m, 3103s	2435s, 2416s, 2379m	1531vs
2a	3160m, 3103s	2466m	1577s, 1548s, 1059vs, br
2b	3150m, 3063s	2486m	1562s, 1084vs, br
3a	3160w, 3128m, 2947m	2494m	1557m, 1203vs, 1080vs, br
3b	3152m, 3136m, 2980s, 2944s	2459s	1548w, 1193vs, 1070vs, br
4a	3157s, 3128s, 2953s	2465s	1552w, 1204vs, 1065vs, br
4b	3163m, 3137m, 2984s, 2944s	2466s	1551w, 1194vs, 1083vs, br
	$\nu(\text{NH})$	$\nu_{\text{as}}(\text{NCO})/\nu_{\text{s}}(\text{NCO})$	$\nu(\text{PF}_6)/\text{others}^{\text{a}}$
5a	3390 m, br	1555 vs/1150vs	^e
5b	3389 s, br	1539 vs/1142 vs	^e
6a	3420 vs	1550 vs/1142 vs	840 vs
6b	3411 s	1547 vs/1151 vs	842 vs
7a	3399 m, br	1540 s/1146 s	^e
7b	3405 vs, br	1530 vs/1137 vs	^e
8	3308 m, br ^b 3106 st, br ^c	1550 s/1171 vs	2244 vs ^d
9a	3325 s	1545 vs/1151 vs	^e
9b	3320 s	1545 vs/1160 vs	^e
10a	3415 s	1562 vs/1156 vs	841 vs
10b	3410 s	1550 vs/1162 vs	840 vs
11a	3395 vs	1595 s/1205 s	855 s
11b	3410 s	1550 s/1172 s	840 vs
12a	3435 s	1560 s/1175 s	850 s

^a See text.

^b $\nu(\text{NH})$.

^c $\nu(\text{OH})$.

^d $\nu(\text{NC})$.

^e Not measured.

without prior isolation (Scheme 1). That we actually deal with a free, or better, lithium co-ordinated tricarbene has been proven by the isolation and structural characterization of the solvent-free dimeric binary compound $[\text{Li}(\text{TRIS}^{\text{Et}})]_2$ [8].

In both cases, the anhydrous dichlorides (FeCl_2 , CoCl_2) are employed, i.e. the metals must be oxidized from the +II to the +III state. While iron(II) in contact with the new ligand much to our surprise spontaneously turns into the deep red iron(III) product upon standing overnight, air has to be passed through the cobalt(II)–tricarbene mixture in order to arrive at the stable d⁶ electronic configuration. Here again the oxidation process is accompanied by a pronounced change in color from dark to light green or almost yellow.

It remains unclear what causes the oxidation of iron(II) in an altogether more reducing medium; presumably it is traces of air. All attempts to isolate the neutral 18 electron species $\text{Fe}(\text{II})(\text{TRIS}^{\text{R}})_6$ have failed so far. Electrochemical studies however show that **3b** can be reversibly reduced though at a rather negative potential (cf. Section 4). In this respect, **3b** resembles more $[\text{FeCp}_2^*]^+$ than $[\text{FeCp}_2]^+$ which indicates an exceedingly strong electron-donating power of TRIS^{R} (**B**).

Both, the new triethylated ligand TRIS^{Et} itself and the complexes prepared from it differ markedly in their solubilities from TRIS^{Me} and its complexes. They unlike **3a**, **3b** and **4b** could not be precipitated as tetraphenylborates from their methanolic solutions. Therefore the purification of the products was carried out by recrystallization from methanol (**3a**) and CH_2Cl_2 –ether or CH_2Cl_2 –hexane (**3b**, **4**) to give the tetrafluoroborates which in the case of **3b** and **4** retain one molecule of CH_2Cl_2 in the crystal.

The mass spectra reflect the cationic nature of both the tris(imidazolium)borate starting material and the hexacarbene complexes in that useful data could only be obtained by the pos-FAB method (Section 8). Here **2** gave rise to signals of the monocationic ion pair $[\text{H}_3\text{TRIS}^{\text{R}}-\text{BF}_4]^+$ and the mono-deprotonated $[\text{H}_2\text{TRIS}^{\text{R}}]^+$ which subsequently loses one of the *N*-alkylimidazole substituents. The MS signal pattern is essentially the same for complexes **3** and **4** with $[\text{M}]^+$ representing the base peak which is followed by the splitting off of one or more of the alkylimidazole rings and the loss of an entire TRIS^{R} group.

Little information is provided by the IR spectra (Table 1). With the exception of the B–H stretching vibrations of medium to strong intensity which range

between 2400 and 2500 cm^{-1} , and the very strong $\nu(\text{BF}_4)$ bands at $1070 \pm 15 \text{ cm}^{-1}$ of the counteranion, no other characteristic features can be made out. As noted more often, the so-called ‘carbene vibration’ $\nu_{\text{as}}(\text{N}\overset{\curvearrowright}{\text{C}}\overset{\curvearrowright}{\text{N}})$ is of low intensity and inseparable from the vibrations of the heteroaromatic ring in these cases (cf. Section 5) [9].

Of the ^1H -, ^{13}C - and ^{11}B -NMR spectra of **1**, **2** and **4** (Table 2), — **3a,b** could not be measured due to their paramagnetic nature — solely the ^{13}C carbene signals of **4** about $\delta 180$ are of major interest in that they compare well with the values of complexes of a whole range of other metals of similar electron-rich imidazolin-2-ylidene ligands (see, e.g. Ref. [10]).

3. X-ray structures of **3b** and **4b**

Both structures fully confirm the earlier findings on $[\text{Fe}(\text{III})(\text{TRIS}^{\text{Me}})_2]\text{BPh}_4$ (**C**) [5], viz., metal centers embedded in a practically spherical quasi-cage structure made up of six five-membered heterocycles which are all C-coordinated (Figs. 1 and 3). The approximate S_6

geometry of these complexes is obvious if one chooses the view along the B–M–B axis (Fig. 2); in this representation the ethyl substituents stick out radially arranged slightly above and below an assumed equatorial plane which contains the metal. The Fe–C bond in **3b** (av. 1.994(4) Å) is identical within three standard deviations with that in **C** (av. 1.984(3) Å) for which we had deduced the absence of any metal–ligand multiple bonding, one reason being that even in Fe(0) species — though with competing CO ligands (!) — no metal to N,N' -carbene ligand backdonation occurs [11]. The same arguments apply for the cobalt to carbon bond lengths in **4b** (av. 1.950(5) Å) for which, however, few comparable data exist [12]. One might also note that the average metal to carbon bonds in **3b** and **4b** are somewhat longer than the metal to nitrogen bonds in the ‘isomeric’ bis[hydrotris(pyrazol-1-yl)borate]metal(III) complexes [13,14] which are regarded as clear M–N single bonds, and that the difference is entirely explained by the different atomic radii of $r(\text{C}_{\text{sp}^2}) - r(\text{N}_{\text{sp}^2}) = 0.047 \text{ Å}$ [15].

As regards the sequence of bond lengths within the five-membered heterocycles, we observe some ring dis-

Table 2
 ^1H -, ^{13}C - and ^{11}B -NMR data for compounds **1**–**12**^a

Complex	Solvent	^1H -NMR	^{13}C -NMR	^{11}B -NMR
1	DMSO- d_6	3.10–5.00 (br, 1H, B–H), 6.81 (s, 6H, HC=CH), 7.25 (s, 3H, C2–H)	121.2, 128.7 (HC=CH), 140.3 (C2)	–3.12 ppm (d, B–H), $^1J_{\text{B–H}} = 324 \text{ Hz}$
2a	DMSO- d_6	3.82 (s, 9H, CH_3), 7.51, 7.72 (dt, 6H, HC=CH) 8.81 (s, 3H, C2–H)	35.6 (CH_3), 123.6, 125.2 (HC=CH), 139.9 (C2)	–2.31 (s, BF_4^-), –5.24 (s, br, B–H)
2b	DMSO- d_6	1.42 (t, 9H, $\text{CH}_2\text{–CH}_3$), 4.17 (q, 6H, $\text{CH}_2\text{–CH}_3$), 7.55 (t, 3H, HC=CH), 7.83 (t, 3H, HC=CH), 8.86 (s, 3H, C2–H)	15.6 ($\text{CH}_2\text{–CH}_3$), 44.3 ($\text{CH}_2\text{–CH}_3$), 123.6, 123.7 (HC=CH), 139.1 (C2)	–2.17 (s, BF_4^-), –3.74 (s, br, B–H)
4a	DMSO- d_6	2.05 (s, 18H, CH_3), 7.00 (d, 6H, HC=CH), 7.20 (d, 6H, HC=CH)	33.5 (CH_3), 123.5, 122.9 (HC=CH), 179.9 (C2)	–1.18 (s, B–H), –2.27 (s, BF_4^-)
4b	DMSO- d_6	0.87 (t, 18H, $\text{CH}_2\text{–CH}_3$), 2.02 (q, 12H, $\text{CH}_2\text{–CH}_3$), 7.16 (br, 6H, HC=CH), 7.50 (br, 6H, HC=CH)	14.0 ($\text{CH}_2\text{–CH}_3$), 41.6 ($\text{CH}_2\text{–CH}_3$), 119.7, 123.8 (HC=CH), 184.3 (C2)	–1.39 (s, B–H), –2.29 (s, BF_4^-)
5a	D $_2$ O	3.63 (m, 12H, CH_2), 4.55 (m, 12H, CH_2)	^b	
5b	D $_2$ O	1.45 (d, 18H, CH_3), 3.45 (m, CH_2 , 6H), 3.88 (m, CH_2 , 6H), 5.11 (m, CHMe , 6H)	20.8 (CH_3), 51.9 (C4), 82.9 (C5), 217.0 (C2)	
6b	Acetone- d_6	1.50 (d, 18H, CH_3), 3.48 (m, CH_2 , 6H), 3.99 (m, CH_2 , 6H), 5.20 (m, CHMe , 6H), 7.70 (s, 6H, NH)	21.2 (CH_3), 52.9 (C4), 83.9 (C5), 205.0 (C2)	
7a	Acetone- d_6	3.59 (m, CH_2 , 12H), 4.45 (m, CH_2 , 12H), 6.90, 7.35 (m, 40H, BPh_4^-) 9.35 (s, 6H, NH)	^b	
8	D $_2$ O	3.88 (m, CH_2), 4.80 (m, CH_2)	^b	
9a	D $_2$ O	3.89 (m, CH_2 , 12H), 4.85 (m, CH_2 , 12H)	43.9 (C4), 71.5 (C5), 208.0 (C2), $J_{\text{Rh,C}} = 36.6 \text{ Hz}$	
10a	Acetone- d_6	3.82 (m, CH_2 , 12H), 4.75 (m, CH_2 , 12H), 9.46 (s, 6H, NH)	44.7 (C4), 72.6 (C5), 209.2 (C2), $J_{\text{Rh,C}} = 34.0 \text{ Hz}$	
10b	Acetone- d_6	1.45 (d, CH_3 , 18H), 3.42 (m, CH_2 , 6H), 3.93 (m, CH_2 , 6H), 5.20 (m, CHMe , 6H), 9.34 (s, 6H, NH)	20.1 (CH_3), 50.6 (C4), 82.0 (C5), 220.0 (C2), $J_{\text{Rh,C}} = 36.0 \text{ Hz}$	

^a Chemical shifts, δ , as ppm downfield from solvent as internal standard for ^1H (399.8 MHz)- and ^{13}C (100.5 MHz)-NMR and $\text{BF}_3\cdot\text{Et}_2\text{O}$ as external standard for ^{11}B -NMR (86.7 MHz).

^b Not measured. Complexes **6a**, **7b**, **9b**, **11** and **12** were not measured.

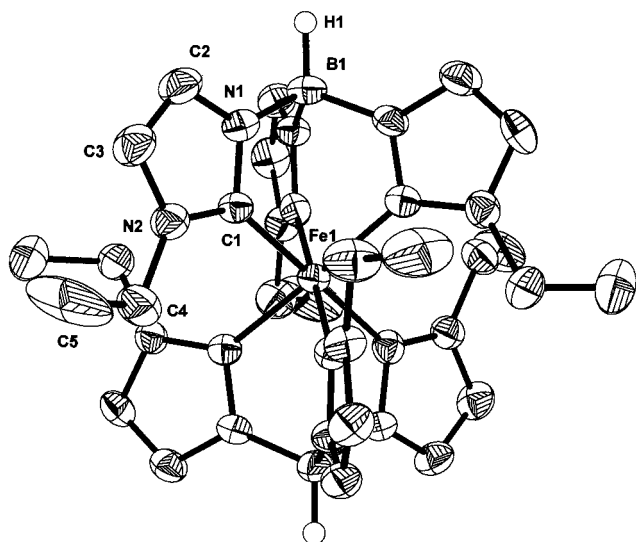


Fig. 1. ORTEP plot and labeling scheme of **3b**. Carbon bound hydrogen atoms, solvent molecule and the BF_4^- -anion have been omitted and only one of six rings is labeled for clarity. The thermal ellipsoids have been drawn to include 50% probability; range of the bond lengths (Å) and angles ($^\circ$): Fe–C_{carbene} 1.983(4)–2.004(3), N–C_{carbene} 1.347(4)–1.371(6), C_{ring}–N_{ring} 1.371(5)–1.396(6), C_{ring}–C_{ring} 1.328(6)–1.344(6), N–B 1.544(6)–1.556(6), C–Fe–C (within one chelating ligand) 87.3(2)–88.2(2), C–Fe–C (between two chelating ligands) 90.7(1)–93.2(2), C–Fe–C (*trans*) 178.1(1)–179.4(2), N–C_{carbene}–N 105.2(4)–106.1(4).

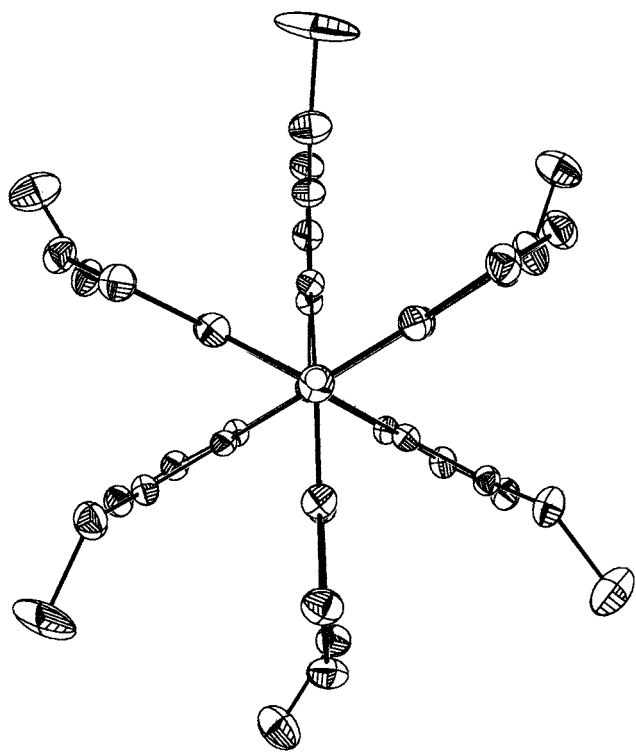


Fig. 2. ORTEP plot of **3b**. View on the highly symmetric ψ - S_6 -cation along the H–B–Fe–B–H-axis.

tortion with short (N–C–N, C–C) and long (N–CC) bonds in the imidazolin-2-ylidene case against very similar bond lengths (C–N, C–C, N–N, 1.37 ± 0.02 Å) in the pyrazolyl rings in complexes of the Trofimenko ligand, a finding which is generally more pronounced and which we used to describe as activation of the heterocycle by the metal [10].

4. Electrochemical studies on **3a,b**

Cyclovoltammetric studies have been performed on the compounds **3a** and **3b** with the intention to learn which oxidation states of the central iron atom are stabilized by the C-cage (Fig. 4, Table 3), and which relations exist between our system, bis[tris(1-pyrazolyl)borate]iron complexes, and the $\text{Fe}(\text{C}_5\text{H}_5)_2$ – $\text{Fe}(\text{C}_5\text{Me}_5)_2$ systems, respectively. Earlier electrochemical studies suggest a close electronic relationship between the $\text{HB}(\text{pz})_3$ (pz = pyrazolyl) and the C_5Me_5 ligand [16] rather than the previously proposed analogy with the unsubstituted C_5H_5 ligand [17].

4.1. Oxidation of **3a,b**

The oxidation wave of **3a** is shown in Fig. 4a. With an anodic peak potential of 0.68–0.93 V_{SCE} depending

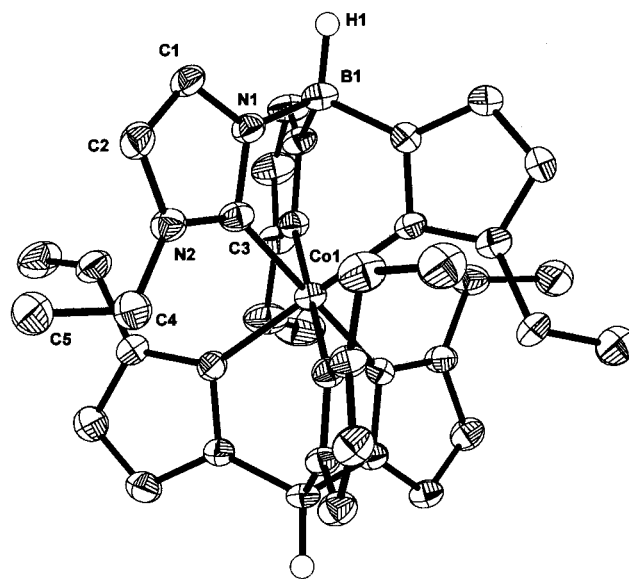


Fig. 3. ORTEP plot and labeling scheme of **4b**. Carbon bound hydrogen atoms, the solvent molecule and the BF_4^- -anion have been omitted and only one of six rings is labeled for clarity. The thermal ellipsoids have been drawn to include 25% probability; range of the bond lengths (Å) and angles ($^\circ$): Co–C_{carbene} 1.943(4)–1.959(5), N–C_{carbene} 1.345(6)–1.378(6), C_{ring}–N_{ring} 1.380(7)–1.392(7), C_{ring}–C_{ring} 1.324(7)–1.355(8), N–B 1.547(8)–1.557(6), C–Co–C (within one chelating ligand) 88.4(2)–88.8(2), C–Co–C (between two chelating ligands) 91.3(2)–91.5(2), C–Co–C (*trans*) 179.7(2)–179.8(2), N–C_{carbene}–N 104.5(4)–105.6(4).

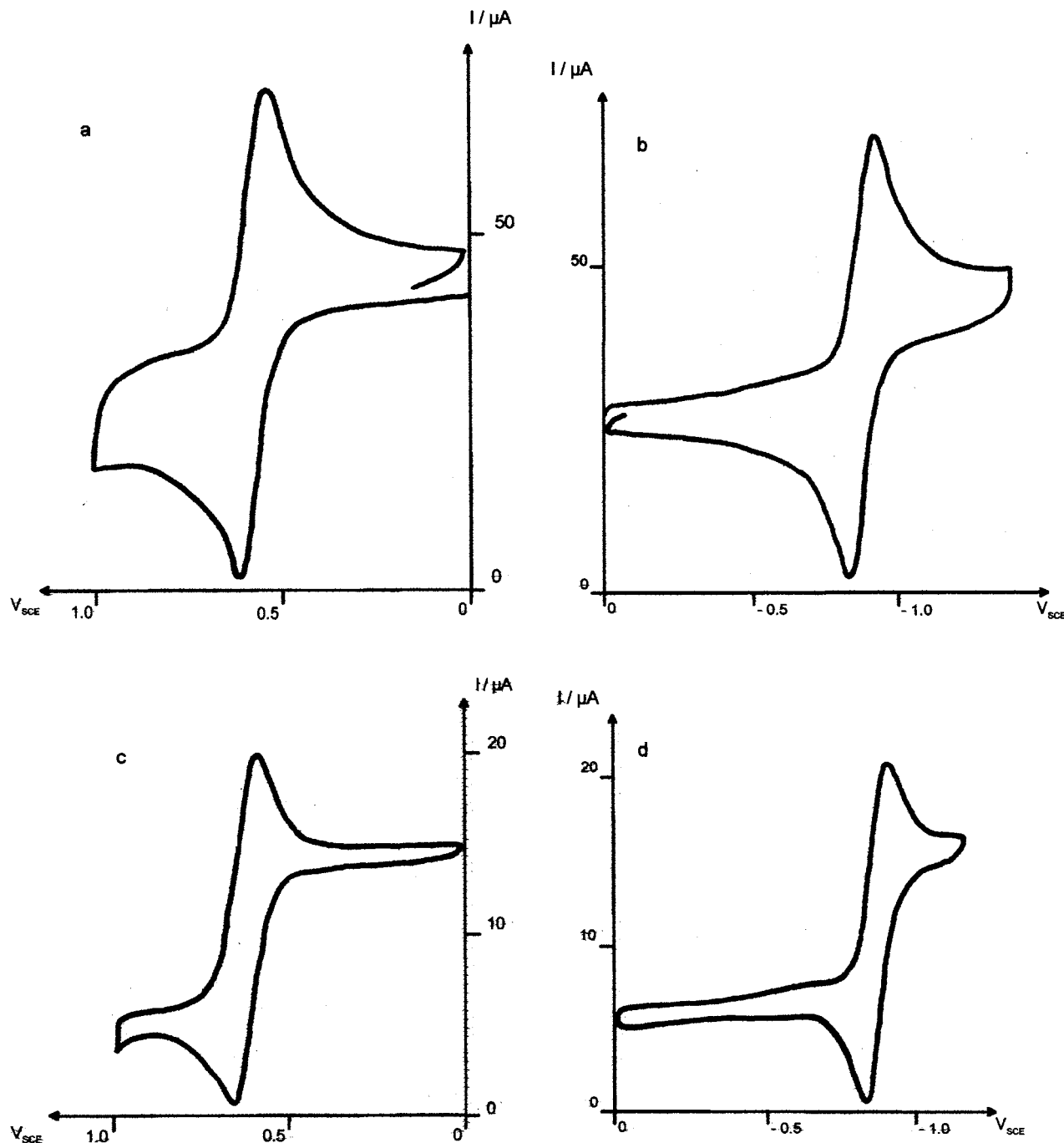


Fig. 4. Cyclic voltammograms of **3a** at a vitreous carbon electrode in acetonitrile (concentration of substrate 2.3×10^{-3} M, 25°C , electrolyte 0.1 M $\text{N}^n\text{Bu}_4[\text{BF}_4]$): (a) oxidation, scan rate 0.2 V s^{-1} ; (b) reduction, scan rate 0.2 V s^{-1} ; (c) oxidation, scan rate 0.02 V s^{-1} ; (d) reduction, scan rate 0.02 V s^{-1} .

on the electrode material and the solvent (sweep rate 0.2 V s^{-1}), the oxidation corresponds to a Nernstian, one electron, electrochemically reversible reaction of $\text{Fe(III)(TRIS}^R)_2^+$ to $\text{Fe(IV)(TRIS}^R)_2^+$. Amazingly, reversibility of this step can even be observed at the much lower sweep rate of 0.02 V s^{-1} (Fig. 4c). For **3b** comparable results were obtained. The controlled potential electrolyses (CPC) of a solution of **3a** in acetonitrile at $1.1 \text{ V}_{\text{SCE}}$ and of **3b** in CH_2Cl_2 at $1.2 \text{ V}_{\text{SCE}}$ gave

both an n_{app} (Faradays mol^{-1} of reactant consumed) close to 1, confirming the one-electron nature of the process. The oxidation results in a change of color of the solutions from red (Fe(III) species) to green (Fe(IV) species). After a complete turnover of the starting material, the Fe(IV)-complexes seemed to be stable in solution for hours under inert conditions. Reduction of the resulting solutions at $-0.4 \text{ V}_{\text{SCE}}$ for **3a** and at $0.3 \text{ V}_{\text{SCE}}$ for **3b** restores the initial oxidation state, which has

been proven by voltammetry at a rotating disc electrode.

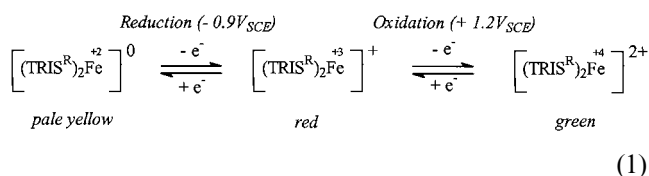
4.2. Reduction of **3a,b**

The reduction wave of **3a** is shown in Fig. 4b. The reduction with a cationic peak potential of -0.80 to -0.87 V_{SCE} depending on measurement conditions also represents a reversible Nernstian, one-electron reaction of $Fe(III)(TRIS^R)_2^+$ to $Fe(II)(TRIS^R)_2$. However, in contrast to the results with **3a**, for **3b** only at a sweep rate of 0.2 $V s^{-1}$ reasonably clear waves are observed. Reversibility of the reduction of **3b** is lost at a scan rate of 0.02 $V s^{-1}$ after two cycles, and the electrode reactions are partially blocked due to a film on the surface. Complex **3a**, on the other hand, shows a fully reversible electrochemical reduction for both sweep rates (Fig. 4d). At the moment, we have no explanation for this difference, unless there was an impurity either in **3b** or in the solvent, or there are solubility differences between the reduced forms of **3a** and **3b**. The CPC of a solution of **3a** in acetonitrile at -1.1 V_{SCE} gave an n_{app} close to 1, confirming the one-electron nature of the reduction. During the reaction the solution changes color from red to pale-yellow, and the precipitation of a pale-yellow solid can be observed. For **3b**, a CPC was performed at -0.9 V_{SCE} in CH_2Cl_2 with comparable results, but no precipitate was obtained, i.e. the neutral reduction product $Fe(II)(TRIS^{Et})_2$ remained in solution completely. For both reduced forms of **3a,b**, an extreme reductive activity towards traces of water or oxygen in the solvent was found in solution. For **3b**, the slow reductive decomposition of the solvent could be observed in the form of a continuous gas evolution during the CPC and after turning off the current; thus, CV measurements showed that a 100% turnover to the reduced $Fe(II)$ species would not occur under these conditions. Complete reoxidation to the red $Fe(III)$ complexes can be achieved by contact with air within a couple of minutes or by a controlled electrochemical oxidation at 0.1 V_{SCE} under inert conditions. In the case of **3a** the precipitate dissolves completely. These results correspond well with

our inability to isolate hexacarbeneiron(II) complexes to date.

4.3. Conclusions

As expected, from an electrochemical point of view compounds **3a,b** show only marginal differences as regards the oxidation and reduction potentials. CV and CPC measurement show that both the oxidized $Fe(IV)$ - and the reduced $Fe(II)$ -complexes are stable under inert conditions (Eq. (1)), i.e. no chemical reaction follows. The latter form seems to be very reactive towards any oxidizing agent. In view of the good solubilities of **3a,b** one can think of an application as homogeneous redox catalysts in electrochemical reactions. On the other hand, we are about to make efforts to isolate both species by means of chemical redox reactions.



5. Syntheses of hexacarbene complexes of $Co(III)$ and $Rh(III)$ via functional isocyanides

In Seebach's term, 2-hydroxyalkylisocyanides are 'masked carbenes', i.e. provide, in combination with electrophilic metals, a perfect source for N,O-carbene complexes of the oxazolidin-2-ylidene type (Eqs. (2) and (3)). At $Pd(II)$ and $Pt(II)$ the tendency of carbene formation from 2-hydroxyalkylisocyanides has been found to be thus strong that most other ligands are removed from the ligand sphere to give rise to only homoleptic tetracarbene complexes (cf. however, Refs. [3a,c]). This synthetic strategy has then been extended to cobalt and rhodium with the intention to obtain hexacarbene complexes. Early attempts with $CoCl_2$ under the usual 'organometallic conditions', i.e. in dried solvents and under an atmosphere of pure nitrogen or argon, only

Table 3

Voltammetric data for **3a,b** at a vitreous carbon electrode (a) and a platinum electrode (b) (electrolyte 0.1 M $N^iBu_4[BF_4]$)

Complex	Solvent	Oxidation		Reduction	
		E_{p_a} ^a	E_{p_c} ^a	E_{p_a} ^a	E_{p_c} ^a
3a	Acetonitrile	(b) 0.68	(b) 0.59	(b) -0.78	(b) -0.87
3b	Acetonitrile	(a) 0.74	(a) 0.62	(a) -0.75	(a) -0.83
		(a) 0.68	(b) 0.60	(b) -0.72	(b) -0.84
	CH_2Cl_2	(a) 0.93	(a) 0.72	(a) -0.67	(a) -0.82
		(b) 0.88	(b) 0.78	(b) -0.68	(b) -0.80

^a V_{SCE} .

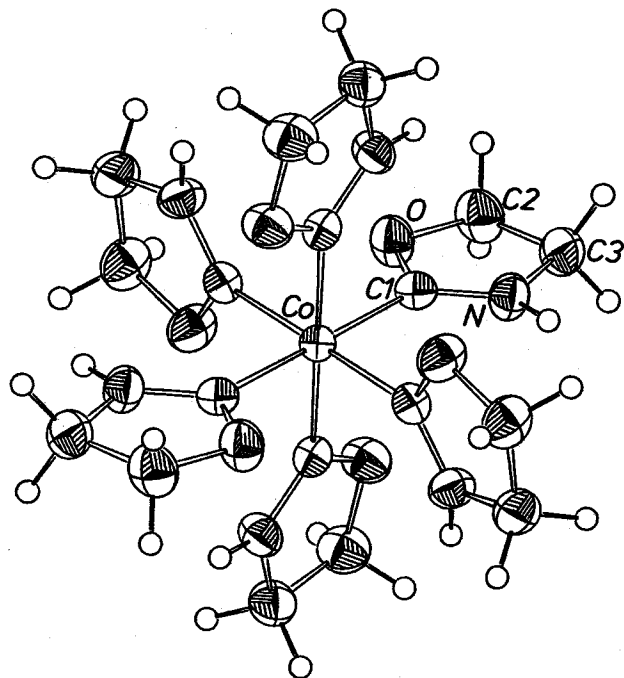


Fig. 5. ORTEP plot and labeling scheme of **5a**. The Cl^- -anions and solvent molecules have been omitted for clarity and the thermal ellipsoids have been drawn to include 25% probability; bond lengths (Å) and angles ($^\circ$): Co–C1 1.937(4), C1–O 1.339(4), O–C2 1.477(6), C2–C3 1.500(5), C3–N 1.473(6), O–C1–N 109.6(3).

Table 4
Bond lengths, hydrogen contacts (Å) and angles ($^\circ$) for **5a**

Co–C1	1.937(4)	Co–C1–O	120.2(2)
		Co–C1–N	130.2(3)
C1–O	1.339(4)	O–C1–N	109.6(3)
O–C2	1.477(6)	C1–O–C2	110.3(3)
C2–C3	1.500(5)	O–C2–C3	104.7(3)
C3–N	1.473(6)	C2–C3–N	100.9(3)
N–C1	1.295(4)	C3–N–C1	114.4(3)
N–HN	0.93(1)		
C2–H2A	0.93(1)	C3–N–H	119.6(3)
C2–H2B	1.03(2)	C1–N–H	125.8(4)
C3–H3A	1.03(2)		
C3–H3B	1.05(1)		
H–bonds ^a			
Cl \cdots H(N) ^I	2.27	Cl \cdots H3A ^{IV}	2.79
Cl \cdots H(N) ^{II}	2.27	Cl \cdots H3A ^V	2.79
Cl \cdots H(N) ^{III}	2.27	Cl \cdots H3A ^{VI}	2.79

^a Roman numerals describe the following symmetrically equivalent positions: I: 1–x, 1–y, 1–z; II: y, y–x, 1–z; III: 1+x–y, x, 1–z; IV: 1+x, y, z; V: 1–x, 1+x–y, z; VI: y–x, –x, z.

First experiments with $\text{RhCl}_3 \cdot 3\text{H}_2\text{O}$ and 2-hydroxyethyl isocyanide in methanol resulted in a pink precipitate which was only soluble in water and analyzed as $\text{RhCl}_3(\text{L}_4)$ where L stands for both, the open-chain functional isocyanide and the cyclic N,O-carbene. In fact, the IR spectrum shows the characteristic absorp-

tions of both species which obviously co-exist in the ligand sphere (Table 1), and conductivity measurements prompt us to describe the complex as **8** with *n* unspecified. That only partial intraligand cyclization occurred presumably comes from the rapid precipitation of the product; a reduction of Rh(III) to Rh(I) on which the carbene formation would be less favorable can be excluded on account of the high frequency of the ($\text{C}\equiv\text{N}$ (isocyanide)) stretching vibration [18].

From these experiences it had become clear that (a) we had to do the reaction in water; (b) use a slight excess of the hydroxyisocyanide; and (c) force complete intraligand cyclization by heating the mixture while bubbling air through it. Under these conditions the originally deep red solution went colorless within 1 h, and the desired hexacarbene rhodium(III) complexes **9a,b** and, after anion exchange, **10a,b** resulted in high yields. According to the elemental analyses, DTA studies and conductivity measurements, the overall composition and nature of these products is amazingly similar to that of the cobalt system (see above and Section 8). This, of course, also holds for the IR spectra where the more asymmetric, largely saturated oxazolidin-2-ylidene ring, unlike the more symmetric and aromatic imidazolin-2-ylidene moiety (cf. Section 2), gives rise to strong or very strong and broad 'carbene absorptions', viz., the antisymmetric and symmetric ($\text{N}\overset{\sim}{\text{C}}\overset{\sim}{\text{O}}$) stretching vibrations about 1550 and 1170 cm^{-1} , respectively (Table 1).

In the ^1H -NMR (recorded in D_2O) of the unsubstituted hexakis(oxazolidin-2-ylidene) complexes **5a**, **6a**, **9a** and **10a**, one observes the typical pattern of an AA'BB' system, while the expected ABX signal pattern with coupling constants similar to those found in the corresponding tetracarbene palladium and platinum complexes [3] appears in the case of the 5-methyl derivatives **5b**, **6b**, **9b** and **10b** (Table 2). No attempt was made to recover any information about the number and/or quantity of stereoisomers or diastereomers which may have formed with the 2-hydroxypropyl isocyanide. The $^{13}\text{C}\{^1\text{H}\}$ -NMR signals of the carbene carbon atoms of the cobalt complexes appear around $\delta 200$ – 220 , i.e. have experienced a low field-shift of some 20–30 ppm as compared to those of the hexakis(imidazolin-2-ylidene)cobalt species (cf. Section 2). At rhodium (**10a,b**), the signals in question are doublets at $\delta 210$ with a coupling constant of 36 Hz, thus providing further evidence for metal–carbon bonding (Table 2).

6. X-ray structure of **5a**

Due to the high symmetry of the crystal — the central cobalt atom resides on a crystallographic 3 bar axis — only one carbene ligand had to be located. The other five are then generated by this symmetry element.

Fig. 5 gives a view of the complex cation together with the atomic numbering scheme. The bonding parameters within the heterocycle differ only marginally from those determined in $[\text{Pd}(\text{CN}(\text{H})\text{CH}_2\text{CH}_2\text{O})_4]\text{Cl}_2$ (**D**) [3c] and related moieties (Table 4). The cobalt to carbene carbon bonds (1.937(4) Å) are somewhat shorter than those in **7a** (1.95(1) Å), yet lie still in the range of $\text{Co}-\text{C}_{\text{sp}^2}$ single bonds as deduced from the respective covalent radii 1.22 Å (Co) and 0.72 Å (C_{sp^2}). This is in accordance with a description of the carbene ligand as a pure σ -donor, an interpretation supported by numerous other observations and findings. The conformational arrangement of the six ligands about the metal is such that in each of the three mutually perpendicular coordination planes the carbenoid heterocycles are alternately coplanar and perpendicular, i.e. all *trans*-positioned heterocycles are coplanar, all *cis* perpendicular. This explains why our attempts to link neighboring carbenes via their NH groups failed (cf. Section 5). Note that in **D** the oxazolidinylidene rings are also rotated with respect to the PdC_4 plane by about 70° . In both cases, **D** and **5a** strong hydrogen bonds to the chloride anions have been established. While, however, in **D** we deal more or less with discrete $[\text{Pd}(\text{CN}(\text{H})\text{CH}_2\text{CH}_2\text{O})_4]\text{Cl}_2$ molecules, a complex three-dimensional network of H-bonding exists in **5a**. Thus, the chloride anion at $[x/a = 2/3, y/b = 1/3, z/c = 0.4695]$ bridges three hexacarbene cobalt cations via very short $\text{Cl}\cdots\text{H}(\text{N})$ -distances (2.27 Å, Table 4). These hydrogen bonds form a trigonal pyramid with Cl^- residing 1.08 Å above or, respectively, below the equilateral triangle. As the same chloride is also at the apex of a second, though essentially more stretched trigonal pyramid made up of $\text{Cl}\cdots\text{H}(\text{C}3)$ contacts, its coordination geometry is that of a strongly distorted octahedron (Fig. 6). The related position at $[2/3, 1/3, 0.2363]$ is occupied half by Cl^- and half by oxygen (from crystal water). Both hydrogen acceptors link three complex

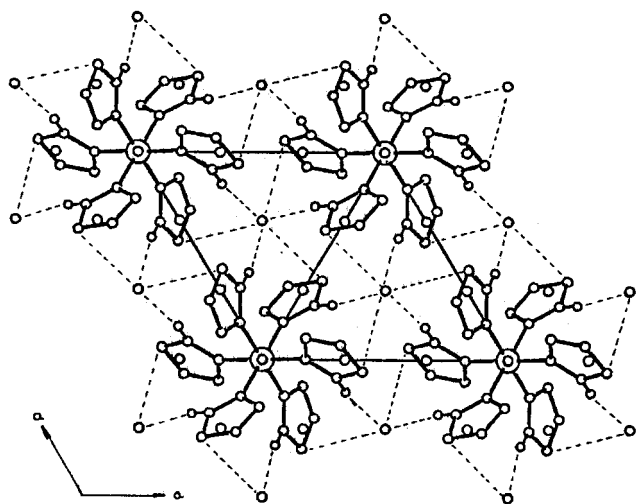


Fig. 6. Elementary cell of **5a**, showing the chloride–hydrogen contacts at 2.27 Å.

cations via $\text{X}\cdots\text{H}(\text{C}2)$ contacts (at an average distance of 2.99 Å) plus three of the water molecules which are incorporated in the crystal lattice ($d(\text{H}\cdots\text{O}2)_{\text{av}} = 2.93$ Å); in addition, three more $\text{X}\cdots\text{H}(\text{C}3)$ (av. 2.80 Å) and various $\text{O}1(\text{H}_2\text{O})\cdots\text{H}(\text{C}2)$ (av. 2.87 Å) interactions occur with adjacent cationic layers.

7. Attempted syntheses of hexacarbene platinum(IV) and chromium(III) complexes

Platinum(IV) complexes with C-ligands including carbenes are well-known and remarkably stable [19,20]. In view of (a) the pronounced donor potentials of the *N,N*- (cf. Section 2) and *N,O*-carbenes which correspond favorably to metals in rather high oxidation states, and (b) the overall stability of the $5d^6$ electron configuration, a hexacarbeneplatinum(IV) species absolutely appeared within reach. Following the successful synthetic approach to the cobalt and rhodium systems (cf. Section 5) we started from hexachloroplatinate in hot aqueous solution which on addition of the 2-hydroxyalkylisocyanides almost immediately turned colorless. Anion exchange with ammonium hexafluorophosphate resulted in the growth of white crystals which according to conductivity data and elemental analyses can be formulated as **11a,b**. DTA measurements on **11a** show that above 214°C mass fragments equivalent to two oxazolines each are cleaved off in three consecutive steps. The IR spectra of **11a,b** show the typical $\nu_{\text{as}}[\text{N}\cdots\text{C}\cdots\text{O}]$ (1590 cm^{-1}) and $\nu_{\text{s}}[\text{N}\cdots\text{C}\cdots\text{O}]$ (1195 cm^{-1}) absorption pattern of oxazolidin-2-ylidene complexes though at markedly higher wavenumbers than that of the tetracarbeneplatinum(II) analogues ($1560, 1160\text{ cm}^{-1}$) (Table 1). Notice, however, that exactly these products are obtained from the attempted recrystallization of **11a,b** from acetone, i.e. some kind of reductive elimination must have occurred which certainly deserves a more thorough investigation.

By a similar preparative route, $\text{CrCl}_3 \cdot 6\text{H}_2\text{O}$ has been converted into orange crystals which due to IR, conductivity and analytical data are tentatively assigned the structural formulae **12a,b** (Section 8) (Eqs. (4) and (5)).

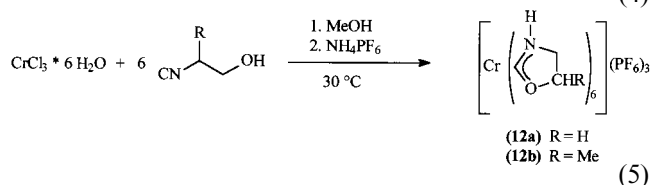
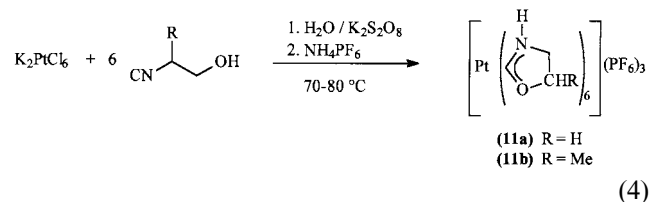


Table 5
Analytical and other data

Complex	Molecular weight (g mol ⁻¹)	Melting point (dec.) (°C)	Yield (%)	Analyses (%)	C	H	N
1	C ₉ H ₁₀ BKN ₆ 252.12	>250	63	(Calc.) (Found)	42.87 42.47	4.00 4.12	33.33 32.89
2a	C ₁₂ H ₁₉ B ₃ F ₈ N ₆ 431.74	133	72	(Calc.) (Found)	33.38 33.02	4.44 3.94	19.47 19.26
2b	C ₁₅ H ₂₅ B ₃ F ₈ N ₆ 473.82	125	75	(Calc.) (Found)	38.02 37.75	5.32 5.40	17.74 17.64
3a	C ₂₄ H ₃₂ B ₃ F ₄ FeN ₁₂ 652.86	>250	69	(Calc.) (Found)	44.15 43.37	4.94 4.43	25.74 25.00
3b	C ₃₀ H ₄₄ B ₃ F ₄ FeN ₁₂ ·CH ₂ Cl ₂ 737.03	>250	50	(Calc.) (Found)	45.30 44.59	5.64 5.81	20.45 19.66
4a	C ₂₄ H ₃₂ B ₃ CoF ₄ N ₁₂ ·CH ₂ Cl ₂ 740.88	230 (dec.)	72	(Calc.) (Found)	40.53 39.16	4.63 4.42	22.69 22.40
4b	C ₃₀ H ₄₄ B ₃ CoF ₄ N ₁₂ ·CH ₂ Cl ₂ 825.04	232 (dec.)	62	(Calc.) (Found)	45.13 45.11	5.62 5.76	20.37 20.56
5a	C ₁₈ H ₃₀ Cl ₃ CoN ₆ O ₆ ·5H ₂ O 681.66	186 (dec.)	75	(Calc.) (Found)	31.72 31.61	5.91 5.88	12.33 12.04
5b	C ₂₄ H ₄₂ Cl ₃ CoN ₆ O ₆ ·5H ₂ O 765.80	208 (dec.)	70	(Calc.) (Found)	37.64 37.55	6.84 6.82	10.97 10.88
6a ^a	C ₁₈ H ₃₀ CoF ₁₈ N ₆ O ₆ P ₃ 920.11	151 (dec.)	100	(Calc.) (Found)	23.50 23.55	3.29 3.29	9.13 8.94
6b	C ₂₄ H ₄₂ CoF ₁₈ N ₆ O ₆ P ₃ 1004.27	171 (dec.)	100	(Calc.) (Found)	28.70 28.93	4.21 4.92	8.37 8.49
7a	C ₆₆ H ₇₀ B ₂ CoN ₆ O ₆ 1147.42	169 (dec.)	65	(Calc.) (Found)	69.09 70.35	6.15 6.82	7.32 6.88
7b	C ₇₂ H ₈₂ B ₂ CoN ₆ O ₆ 1207.87	174 (dec.)	65	(Calc.) (Found)	71.60 72.93	6.84 7.50	6.96 6.73
8	C ₁₃ H ₂₈ Cl ₃ N ₄ O ₇ Rh 561.61	136 (dec.)	95	(Calc.) (Found)	27.80 27.81	5.02 4.77	9.98 9.97
9a	C ₁₈ H ₃₀ Cl ₃ N ₆ O ₆ Rh·5H ₂ O 725.55	118 (dec.)	80	(Calc.) (Found)	29.79 29.66	5.55 5.44	11.58 11.83
9b	C ₂₄ H ₄₂ Cl ₃ N ₆ O ₆ Rh·5H ₂ O 809.75	241 (dec.)	80	(Calc.) (Found)	35.60 35.42	6.47 6.53	10.38 10.48
10a	C ₁₈ H ₃₀ F ₁₈ N ₆ O ₆ P ₃ Rh 964.14	229 (dec.)	80	(Calc.) (Found)	22.42 22.75	3.14 2.75	8.72 8.86
10b	C ₂₄ H ₄₂ F ₁₈ N ₆ O ₆ P ₃ Rh 1048.27	229 (dec.)	95	(Calc.) (Found)	27.50 27.78	4.04 4.10	8.02 8.00
11a	C ₁₈ H ₃₀ F ₂₄ N ₆ O ₆ P ₄ Pt 1201.24	215 (dec.)	90	(Calc.) (Found)	18.00 18.02	2.52 2.58	7.00 6.79
11b	C ₂₄ H ₄₂ F ₂₄ N ₆ O ₆ P ₄ Pt 1285.52	200 (dec.)	90	(Calc.) (Found)	22.42 22.57	3.29 3.50	6.54 6.53
12a	C ₁₈ H ₃₀ CrF ₁₈ N ₆ O ₆ P ₃ 913.2	120	50	(Calc.) (Found)	23.67 24.16	3.31 4.02	9.20 8.65
12b	C ₂₄ H ₄₂ CrF ₁₈ N ₆ O ₆ P ₃ 997.36	165	50	(Calc.) (Found)	28.90 30.38	4.24 4.56	8.43 8.28

^a Co: Calc./Found 6.40/6.53; P: Calc./Found 10.1/10.2.

Work is in progress to further confirm these results and to explore the limitations on the part of the metals to form poly- and percarbene complexes, particularly with the TRIS^R ligand.

8. Experimental

All operations were carried out under an atmosphere of dry argon using Schlenk-tube and vacuum techniques. Glassware was dried with a heat-gun in high-vacuum. The organic solvents were dried (using

standard procedures [21]), distilled and stored under argon. IR spectra were run on a Nicolet 520 FT-IR, a Zeiss IMR-16, a Zeiss IMR-25, and a Beckmann IR12 spectrometer. Microanalyses (C, H, N) (Table 5) were obtained with a Heraeus VT CHN-O-Rapid Element-analysator. Mass spectra were obtained with a Finnigan MAT 90 using the FAB technique (matrix: *m*-nitrobenzylalcohol). ¹H-, ¹³C- and ¹¹B-NMR spectra were recorded on a JEOL GSX 270, a JEOL EX 400, a JEOL FX90Q, and a JEOL JNM-C-60HL. Conductivity measurements were performed on LBR (WTW, Weilheim) and LF39, WTW D 812, DTG/DTA mea-

surements on a Mettler Thermoanalyzer. UV–vis spectra were run on a Beckmann UV 5270 and analyzed using a du Pont 310 Curve Resolver.

Imidazole, KBH_4 , FeCl_2 , CoCl_2 , trialkyloxonium–tetrafluoroborates and *n*-BuLi were purchased from Aldrich, Fluka or Merck. Imidazole was purified by sublimation and stored under argon prior to use. The isocyanides $\text{CNCH}_2\text{CHROH}$ ($\text{R} = \text{H, Me}$) were prepared by a published method [3].

The electrochemical studies were carried out at room temperature (r.t.). Conventional electrochemical equipment was used for cyclic voltammetry (EGG PAR model 362 scanning potentiostat with an XY recorder). The solutions of the compounds were deaerated and saturated with nitrogen. Acetonitrile and CH_2Cl_2 were purchased from SDS. $\text{N}^m\text{Bu}_4[\text{BF}_4]$ (purum) from Fluka was recrystallized twice from ethanol–water prior to use in order to eliminate traces of iodide completely.

For both, cyclic voltammetry (CV) and voltammetry at a rotating electrode (speed: 2000 rpm), the working electrode was a freshly polished disc of vitreous carbon (diameter 3 mm) or of platinum (diameter 2 mm). All potentials refer to the saturated calomel electrode (SCE) and have not been corrected for the ohmic drop (*IR*).

Controlled potential electrolyses (CPC) were carried out in a batch cell [22] at a platinum electrode (diameter 2.2 cm) for **3a** and at a vitreous carbon electrode (diameter 4.0 cm) for **3b**. CPC reactions were followed by voltammetry at a rotating electrode (scan rate 0.1 V s^{-1}) and CV (scan rate 0.2 V s^{-1}) at a vitreous carbon electrode. Solutions (20 ml) of the substrates at concentrations of about $3 \times 10^{-3} \text{ M}$ in acetonitrile and CH_2Cl_2 were prepared under nitrogen. The concentration of the base electrolyte $\text{N}^m\text{Bu}_4[\text{BF}_4]$ was 0.1 M.

8.1. Preparation of potassium hydrotris(1-imidazolyl)borate (**1**)

Caution: Since large amounts of hydrogen are evolved, the reaction should be run in an efficient hood. Open flames or sparks must be avoided completely.

In a long Schlenk tube, 15.05 g (0.220 mol) of freshly sublimed and ground imidazole are mixed with 3.98 g (0.074 mol) of ground KBH_4 under argon with stirring, and the tube is connected to a volumetric device. The Schlenk tube is then placed in an oil bath which is slowly heated to 90°C , and the mixture is allowed to melt. At this point the hydrogen evolution starts and the temperature is raised gradually but not over 185°C to maintain a steady controlled evolution of hydrogen. When about 5 l (0.220 mol) of hydrogen have been evolved, the melt gets viscous, and the evolution of hydrogen stops. Heating is removed and the crude product is allowed to cool to r.t. under vacuum to form a porous, glasslike white solid which is treated with 10

ml of cold dry THF with stirring. The resulting white suspension is filtered under continuous cooling to give white, microcrystalline, hygroscopic potassium hydrotris(1-imidazolyl)borate (**1**) which is washed with another 10 ml of dry cold THF and $2 \times 30 \text{ ml}$ of dry diethylether to give after drying in vacuum the analytically pure product.

8.2. Preparation of hydrotris(3-methyl-imidazolium-1-yl)borate bis(tetrafluoroborate) (**2a**) and hydrotris(3-ethyl-imidazolium-1-yl)borate bis(tetrafluoroborate) (**2b**)

In a Schlenk tube trimethyloxonium tetrafluoroborate or, respectively, triethyloxonium tetrafluoroborate (9.60 mmol, 20% excess) is dissolved in 30 ml of dry CH_2Cl_2 , and 2.0 g (7.93 mmol) of **1** is added in small portions with stirring to give a white suspension. Stirring is continued overnight, and the solvent is decanted to leave a white slurry. The crude products are washed with $2 \times 10 \text{ ml}$ of dry EtOH followed by $2 \times 30 \text{ ml}$ of dry diethylether. After drying in vacuum, **2a** and **2b** result as white, microcrystalline, hygroscopic solids which according to the elemental analyses still contain one equivalent of KBF_4 . Analytically pure tris(imidazolium)borates can be obtained as large, colorless prisms by recrystallizing the compounds from boiling methanol.

2a: MS [$\text{M} = (\text{TRIS}^{\text{Me}})^{2+}$] (FAB, Xe, *m*-NBA, (*m/z* (rel. intensity))): 345 (100) [$\text{M} + \text{BF}_4^-$] $^+$, 257 (47) [$\text{M} - \text{H}$] $^+$, 175 (57) [$\text{M} - \text{H} - \text{C}_4\text{H}_6\text{N}_2$] $^+$. **2b:** MS [$\text{M} = (\text{TRIS}^{\text{Et}})^{2+}$] (FAB, Xe, *m*-NBA, (*m/z* (rel. intensity))): 387 (100) [$\text{M} + \text{BF}_4^-$] $^+$, 299 (50) [$\text{M} - \text{H}$] $^+$, 203 (75) [$\text{M} - \text{H} - \text{C}_4\text{H}_6\text{N}_2$] $^+$.

8.3. Preparation of the bis[hydrotris(3-alkyl-imidazolium-2-ylidene-1-yl)borate]iron(III) tetrafluoroborates (**3a**) and (**3b**)

A 1.6 M solution of *n*-BuLi in hexane (3.0 ml, 4.82 mmol) is added dropwise with stirring to a suspension of 1.60 mmol of **2a** (or **2b**) in 50 ml of dry THF at -78°C . The suspension is stirred overnight and allowed to warm to r.t. to give a light yellow suspension. The mixture is again cooled to -78°C , and 101 mg (0.80 mmol) of anhydrous FeCl_2 are added in portions with stirring to give a yellow suspension which changes color to deep red when being allowed to warm to r.t. overnight. The solvent is removed in vacuum and the residue extracted with $2 \times 30 \text{ ml}$ of dry CH_2Cl_2 . The resulting mixture is filtered, and the filtrate is concentrated in vacuum. Addition of 30 ml of dry hexane causes the products to precipitate; after drying in high vacuum **3a** and **3b** remain as red powders. Further purification can be achieved by recrystallization from CH_2Cl_2 – Et_2O .

3a: MS (FAB, Xe, *m*-NBA, (*m/z* (rel. intensity)): 566 (100) $[M]^+$, 485 (6) $[M - C_4H_5N_2]^+$, 311 (9) $[M - TRIS^{Me}]^+$. **3b:** MS (FAB, Ar, *m*-NBA, (*m/z* (rel. intensity)): 650 (100) $[M]^+$, 555 (5) $[M - C_5H_7N_2]^+$, 353 (9) $[M - TRIS^{Et}]^+$.

8.4. Preparation of the bis[hydrotris(3-alkyl-imidazolin-2-ylidene-1-yl)borate]cobalt(III) tetrafluoroborates (**4a**) and (**4b**)

The procedure is essentially the same as that for **3a** or **3b**, respectively. Anhydrous $CoCl_2$ (104 mg, 0.80 mmol) is added with stirring to obtain a light green suspension which changes to dark green during the warm-up phase to r.t. overnight. The reaction mixture is oxidized by allowing air to pass through for 2 h after which time a light yellow–green suspension has formed. The solvent is removed in vacuum and the residue is extracted into 2×30 ml of dry CH_2Cl_2 . The resulting mixture is filtered, and the filtrate is concentrated in vacuum. On addition of 30 ml of dry hexane the crude products **4a** (**4b**) precipitate. Filtration and drying in high vacuum yield yellow to green powders. As with **3a** (**3b**), further purification can be achieved by recrystallization from $CH_2Cl_2-Et_2O$.

4a: MS (FAB, Ar, *m*-NBA, (*m/z* (rel. intensity)): 569 (100) $[M]^+$, 488 (5) $[M - C_4H_5N_2]^+$, 314 (18) $[M - TRIS^{Me}]^+$. **4b:** MS (FAB, Xe, *m*-NBA, (*m/z* (rel. intensity)): 653 (100) $[M]^+$, 558 (3) $[M - C_5H_7N_2]^+$, 356 (13) $[M - TRIS^{Et}]^+$, 232 (17) $[M - Et - C_5H_7N_2 - TRIS^{Et}]^+$.

8.5. Preparation of hexakis(oxazolidin-2-ylidene)-cobalt(III)-chloride-pentahydrate (**5a**) and hexakis(5-methyloxazolidin-2-ylidene)cobalt(III)-chloride-pentahydrate (**5b**)

To a solution of 0.69 g (2.90 mmol) of $CoCl_2 \cdot 6H_2O$ in 15 ml of ethanol 1.24 g (17.4 mmol) of 2-isocyan ethanol or, respectively, 1.48 g (17.4 mmol) of 1-isocyanopropan-2-ol are added dropwise. The mixture is heated to 40–50°C, and air is bubbled through the solution causing the color to change from green via red and orange to yellow. After 3 h the solution is concentrated and acetone is carefully added whereby a white solid precipitates. The precipitate is filtered off, washed three times with 5 ml of acetone each and dried in high vacuum. Recrystallization from water yields **5a,b** as colorless hexagonal prisms. Hygroscopic materials from which the crystal water has been removed result from drying **5a,b** in vacuo at 80°C. Molar conductivities of **5a** [2]; **5b:** A_M (22°C, 10^{-7} M, H_2O) = $293 \Omega^{-1} mol^{-1} cm^2$. UV–vis (22°C, H_2O); **5a:** λ_{max} = 295 nm, ϵ = $338 l cm^{-1} mol^{-1}$.

DTA measurements on **5a** indicate a 10.75% loss of weight up to 150°C which is the equivalent of five molecules of water.

8.6. Preparation of hexakis(oxazolidin-2-ylidene)-cobalt(III)-hexafluorophosphate (**6a**) and hexakis(5-methyloxazolidin-2-ylidene)cobalt(III)-hexafluorophosphate (**6b**)

To 2.90 mmol of **5a** or **5b** in water, 1.42 g (8.70 mmol) of NH_4PF_6 is added. A white solid precipitates which is filtered off, washed with 5×10 ml of water and dried in high vacuum. Further purification is possible by recrystallization from acetone to give **6a,b** as small octahedral crystals.

Molar conductivities of **6a:** A_M (22°C, 10^{-7} M, acetone) = $200 \Omega^{-1} mol^{-1} cm^2$, A_M (22°C, 10^{-7} M, nitromethane) = $253 \Omega^{-1} mol^{-1} cm^2$; **6b:** A_M (22°C, 10^{-7} M, acetone) = $327 \Omega^{-1} mol^{-1} cm^2$, A_M (22°C, 10^{-7} M, nitromethane) = $244 \Omega^{-1} mol^{-1} cm^2$.

8.7. Preparation of (Δ^2 -oxazolin-2-ato)pentakis(oxazolidin-2-ylidene)cobalt(III)-tetraphenylborate (**7a**) and (5-methyl- Δ^2 -oxazolin-2-ato)pentakis(5-methyl-oxazolidin-2-ylidene)cobalt(III)-tetraphenylborate (**7b**)

To 2.90 mmol of **5a** or **5b** in methanol is added 3.01 g (8.80 mmol) of $NaBPh_4$. A white solid precipitates which is filtered off, washed with 10×10 ml of water and dried in high vacuum. Further purification is possible by recrystallization from acetone to give **7a,b** as colorless needles.

Molar conductivities of **7a:** A_M (22°C, 10^{-7} M, acetone) = $229 \Omega^{-1} mol^{-1} cm^2$, A_M (22°C, 10^{-7} M, nitromethane) = $137 \Omega^{-1} mol^{-1} cm^2$; **7b:** A_M (22°C, 10^{-7} M, acetone) = $285 \Omega^{-1} mol^{-1} cm^2$.

8.8. Preparation of the mixed isocyanoethanol(oxazolidin-2-ylidene)rhodium(III) complex (**8**)

To a solution of 0.13 g (0.48 mmol) of $RhCl_3 \cdot 3H_2O$ in 20 ml of methanol 0.16 g (1.92 mmol) of 2-isocyan ethanol is added. Immediately a pink solid precipitates which is filtered off, washed with 3×10 ml of diethylether and dried in high vacuum. For further purification the compound can be recrystallized from acetone–water.

Molar conductivity of **8:** A_M (22°C, 10^{-7} M, H_2O) = $113 \Omega^{-1} mol^{-1} cm^2$.

8.9. Preparation of hexakis(oxazolidin-2-ylidene)-rhodium(III)-chloride-pentahydrate (**9a**) and hexakis(5-methyloxazolidin-2-ylidene)rhodium(III)-chloride-pentahydrate (**9b**)

To a solution of 0.20 g (0.76 mmol) of $RhCl_3 \cdot 3H_2O$ in 30 ml of water is added 0.32 g (4.56 mmol) of

2-isocyanoethanol or 0.39 g (4.56 mmol) of 1-isocyanopropan-2-ol, respectively. The mixture is heated to 50–60°C and air is bubbled through the solution by which the reaction mixture changes color from red–pale yellow. After 6 h the volume is reduced to one half, and acetone is carefully added until a white solid precipitates. The solid is filtered off, washed with 5 × 5 ml of acetone and dried in high vacuum. For further purification the product can be recrystallized from methanol–acetone.

Molar conductivities of **9a**: Λ_M (22°C, 10^{-7} M, H₂O) = 298 Ω^{-1} mol⁻¹ cm²; **9b**: [2].

8.10. Preparation of hexakis(oxazolidin-2-ylidene)-rhodium(III)-hexafluorophosphate (**10a**)

To a solution of 0.20 g (0.76 mmol) RhCl₃·3H₂O in 30 ml of water 0.32 g (4.56 mmol) of 2-isocyanoethanol is added. The mixture is heated to 50–60°C, and 0.37 g (2.28 mmol) NH₄PF₆ is added which causes the solution to immediately turn to pink. Air is bubbled through the solution for at least 2 h after which time the then colorless solution is allowed to cool to r.t. The resulting microcrystalline precipitate is filtered off, washed with 3 × 5 ml of water and dried in high vacuum. Further purification is achieved by recrystallization from acetone–diethylether. For the preparation of hexakis(5-methyloxazolidin-2-ylidene)rhodium(III)-hexafluorophosphate (**10b**) (cf. [2]).

Molar conductivities of **10a**: Λ_M (22°C, 10^{-7} M, acetone) = 366 Ω^{-1} mol⁻¹ cm²; **10b**: Λ_M (22°C, 10^{-7} M, acetone) = 390 Ω^{-1} mol⁻¹ cm², Λ_M (22°C, 10^{-7} M, nitromethane) = 225 Ω^{-1} mol⁻¹ cm².

8.11. Preparation of hexakis(oxazolidin-2-ylidene)-platinum(IV)-hexafluorophosphate (**11a**) and hexakis(5-methyloxazolidin-2-ylidene)platinum(IV)-hexafluorophosphate (**11b**)

A solution of 0.16 g (0.32 mmol) of K₂[PtCl₆] in 40 ml of water are reacted with 0.14 g (1.92 mmol) of 2-isocyanoethanol or, respectively, 0.16 g (1.92 mmol) of 1-isocyanopropan-2-ol. Some K₂S₂O₈ (0.5 g) is added in order to prevent reduction of the metal. Upon heating to 70–80°C the yellow solution decolorizes quickly. After 1 h, 0.21 g (1.28 mmol) of NH₄PF₆ is added and the mixture is allowed to cool to r.t. A white, microcrystalline precipitate forms which is filtered off, washed with 5 × 5 ml of water and dried in vacuum. All attempts to recrystallize the crude products resulted in decomposition of the hexacarbeneplatinum(IV) to the tetrakis(oxazolidin-2-ylidene)platinum(II) species.

Molar conductivity of **11b**: Λ_M (22°C, 10^{-7} M, acetone) = 381 Ω^{-1} mol⁻¹ cm².

8.12. Preparation of hexakis(oxazolidin-2-ylidene)-chromium(III)-hexafluorophosphate (**12a**) and hexakis(5-methyloxazolidin-2-ylidene)chromium(III)-hexafluorophosphate (**12b**)

To a solution of 0.30 g (1.13 mmol) of CrCl₃·6H₂O in 30 ml of methanol 0.48 g (6.78 mmol) of 2-isocyanoethanol or, respectively, 0.58 g (6.78 mmol) of 1-isocyanopropan-2-ol is added dropwise. After addition of 0.55 g (3.39 mmol) of NH₄PF₆ the mixture is warmed to 30°C for 2–3 h. On standing overnight at r.t., orange crystals form which are collected on a frit, washed with 2 × 5 ml of water and dried in high vacuum. Recrystallization occurs from acetone–diethylether.

Molar conductivities of **12a**: Λ_M (22°C, 10^{-7} M, acetone) = 261 Ω^{-1} mol⁻¹ cm²; **12b**: Λ_M (22°C, 10^{-7} M, acetone) = 343 Ω^{-1} mol⁻¹ cm².

8.13. X-ray structure determinations

Single crystals of **3b** were obtained by slow diffusion of hexane into a dichloromethane solution of **3b**, those of **4b** by slow evaporation of the solvent from a methanolic solution. Suitable crystals of **5a** finally grew from isopropanol.

Crystallographic data of **5a** were collected on an STOE diffractometer using Mo–K_α radiation (λ = 0.71073 Å) and a graphite monochromator, those of **3b** and **4b** on a Siemens P4 equipped with a CCD area detector and a LT device (Table 6). The crystals of **3b** and **4b** were covered with perfluoropolyether oil at –40°C and suitable samples selected and mounted on a glass fiber. Cell dimensions were determined from the reflections on 15 frames each on four different χ and ψ settings by changing ψ by 0.3° per frame at 183 K (**3b**) or 193 K (**4b**). Data collection was performed in the hemisphere mode of the SMART program at the same temperature by collecting a total of 1200 frames. Data reduction was performed by the program SAINT; absorption correction was applied with the program SADABS [23]. The structures were solved by direct methods (**3b**) or the Patterson-method (**4b**) using SHELXS-97 [23]. Non-hydrogen atoms were refined anisotropically and hydrogens isotropically in calculated positions using SHELXL-97 [23]. Referring to compounds **3b** and **4b** the B-bonded hydrogen atoms were found by DiffMap and refined freely. For compound **4b** the hydrogen atoms attached of the water molecule could not be located by Diffmap.

Intensity data of **5a** were collected at 20°C with the $\omega/2\theta$ -scan mode. The structure was solved by direct methods using MULTAN-77 [24], IMPAS and X-RAY-76 [25]. With the weighting scheme $w = x \times y$; $x = 1$ for $\sin \theta > B$, $x = \sin \theta / B$ for $\sin \theta \leq B$ ($B = 0.35$); $y = 1$ for $C > |F_o|$, $y = C / |F_o|$ for $C \leq |F_o|$ (45.0) applied to the $\Sigma w ||F_o| - |F_c||^2$ function to be minimized in the refine-

Table 6
Crystal data and structure refinement of **3b**, **4b** and **5a**

Compound	3b	4b	5a
Empirical formula	C ₃₁ H ₄₆ B ₃ Cl ₂ F ₄ FeN ₁₂	C ₃₀ H ₄₄ B ₃ CoF ₄ N ₁₂ O	C ₁₈ H ₄₀ CoCl ₃ N ₆ O ₁₁
Formula weight	821.98	756.13	681.66
Crystal size (mm)	0.4 × 0.3 × 0.2	0.10 × 0.10 × 0.10	0.63 × 0.30 × 0.10 5
Crystal system	Monoclinic	Monoclinic	Trigonal
Space group	<i>P</i> 2 ₁ / <i>c</i>	<i>P</i> 2 ₁ / <i>c</i>	<i>P</i> $\bar{3}$ <i>c</i> 1
<i>a</i> (Å)	13.795(3)	13.5392(17)	8.872(2)
<i>b</i> (Å)	14.405(3)	14.1622(18)	8.872(2)
<i>c</i> (Å)	19.973(5)	19.503(2)	21.562(2)
α (°)	90.00	90.00	90.00
β (°)	106.222(8)	103.667(2)	90.00
γ (°)	90.00	90.00	120.00
<i>V</i> (Å ³)	3811.0(15)	3633.7(8)	1470
<i>Z</i>	4	4	2
<i>D</i> _{calc} (g m ⁻³)	1.433	1.382	1.51(2)
Absorption coefficient (mm ⁻¹)	0.597	0.537	10.28
<i>F</i> (000)	1708	1576	
Temperature (K)	183(2)	193(2)	293
2 θ range for data collection (°)	13.62–49.42	3.10–47.64	5.3–54.1
Index ranges	–16 ≤ <i>h</i> ≤ 16, –15 ≤ <i>k</i> ≤ 15, –23 ≤ <i>l</i> ≤ 23	–15 ≤ <i>h</i> ≤ 15, –16 ≤ <i>k</i> ≤ 16, –21 ≤ <i>l</i> ≤ 21	
Reflections collected	17 805	16 321	
Independent reflections	6011 (<i>R</i> _{int} = 0.0517)	5223 (<i>R</i> _{int} = 0.0539)	1220
Observed reflections	4133 (<i>F</i> > 4 σ (<i>F</i>))	2766 (<i>F</i> > 4 σ (<i>F</i>))	955
Weighting scheme	$w^{-1} = \sigma^2 F_o^2 + (0.0652P)^2 + 7.1081P$ where $P = (F_o^2 + 2F_c^2)/3$	$w^{-1} = \sigma^2 F_o^2 + (P)^2 + P$ where $P = (F_o^2 + 2F_c^2)/3$	
Final <i>R</i> indices [<i>F</i> > 4 σ (<i>F</i>)]	<i>R</i> ₁ = 0.0673, <i>wR</i> ₂ = 0.1501	<i>R</i> ₁ = 0.0665, <i>wR</i> ₂ = 0.1702	<i>R</i> ₁ = 0.052
<i>R</i> indices (all data)	<i>R</i> ₁ = 0.1067, <i>wR</i> ₂ = 0.1730	<i>R</i> ₁ = 0.1249, <i>wR</i> ₂ = 0.2050	<i>R</i> ₁ = 0.056
Goodness-of-fit on <i>F</i> ²	1.055	0.950	
Largest difference peak (e Å ⁻³)	0.387	1.053	

ment process the positional parameters of all hydrogen atoms of the carbenoid heterocycles could be determined. No efforts were made to locate the hydrogens of the water molecules incorporated in the lattice.

9. Supplementary material

Crystallographic data for the structural analysis have been deposited with the Cambridge Crystallographic Data Centre, CCDC no. 147 028 for compound **3b** and CCDC no. 147 029 for compound **4b**. Copies of this information can be obtained free of charge from The Director, CCDC, 12 Union Road, Cambridge CB2 1EZ, UK (fax: +44-1223-336033, e-mail: deposit@ccdc.cam.ac.uk or www: <http://www.ccdc.cam.ac.uk>).

Acknowledgements

Financial support for this work by the Fonds der Chemischen Industrie, the Deutsche Forschungsge-

meinschaft and the BAYER AG is gratefully acknowledged. We also thank Professor Joachim Fuchs and Professor Hans Hartl of the Institut für Anorganische und Analytische Chemie der Freien Universität Berlin for their help in the X-ray structure determinations.

References

- [1] D. Bourissou, O. Guerret, F.P. Gabbaï, G. Bertrand, Chem. Rev. 100 (2000) 39.
- [2] U. Plaia, H. Stolzenberg, W.P. Fehlhammer, J. Am. Chem. Soc. 107 (1985) 2171.
- [3] (a) K. Bartel, W.P. Fehlhammer, Angew. Chem. 86 (1974) 588. (b) K. Bartel, W.P. Fehlhammer, Angew. Chem. Int. Ed. Engl. 13 (1974) 599. (c) U. Plaia, W.P. Fehlhammer, Z. Naturforsch. 41b (1986) 1005. (d) W.P. Fehlhammer, K. Bartel, U. Plaia, A. Völkl, A.T. Liu, Chem. Ber. 118 (1985) 2235. (e) W. P. Fehlhammer, K. Bartel, B. Weinberger, U. Plaia, Chem. Ber. 118 (1985) 2200. (f) W.P. Fehlhammer, D. Achatz, U. Plaia, A. Völkl, Z. Naturforsch. 42b (1987) 720.
- [4] S. Trofimenko, Chem. Rev. 93 (1993) 943.
- [5] U. Kernbach, M. Ramm, P. Luger, W.P. Fehlhammer, Angew. Chem. Int. Ed. Engl. 35 (1996) 310.

- [6] S.A.A. Zaidi, T.A. Khan, S.R.A. Zaidi, Z.A. Siddiqi, *Polyhedron* 4 (1985) 1163.
- [7] (a) S. Trofimenko, *J. Am. Chem. Soc.* 89 (1967) 3170. (b) S. Trofimenko, *Inorg. Synth.* 12 (1970) 99.
- [8] R. Fränkel, C. Birg, U. Kernbach, T. Habereeder, H. Nöth, W.P. Fehlhammer, to be published.
- [9] (a) W.P. Fehlhammer, T. Bliss, J. Fuchs, G. Holzmann, *Z. Naturforsch.* 47b (1992) 78. (b) W.P. Fehlhammer, T. Bliß, W. Sperber, J. Fuchs, *Z. Naturforsch.* 40b (1994) 494.
- [10] (a) D. Rieger, S.D. Lotz, U. Kernbach, S. Schröder, C. André, W.P. Fehlhammer, *Inorg. Chim. Acta* 222 (1994) 275. (b) S.D. Lotz, D. Rieger, U. Kernbach, J. Bertran Nadal, C. André, W.P. Fehlhammer, *J. Organomet. Chem.* 491 (1995) 135. (c) D. Rieger, S.D. Lotz, U. Kernbach, J. Fuchs, W.P. Fehlhammer, *Chem. Ber.* 126 (1993) 2243.
- [11] (a) G. Huttner, W. Gartzke, *Chem. Ber.* 105 (1972) 2714. (b) P.B. Hitchcock, M.F. Lappert, S.A. Thomas, A.J. Thorne, A.J. Carty, N.J. Taylor, *J. Organomet. Chem.* 315 (1986) 27.
- [12] (a) A.W. Coleman, P.B. Hitchcock, M.F. Lappert, R.K. Maskell, J.H. Muller, *J. Organomet. Chem.* 250 (1983) C9. (b) A.W. Coleman, P.B. Hitchcock, M.F. Lappert, R.K. Maskell, J.H. Muller, *J. Organomet. Chem.* 296 (1985) 173. (c) W. David, R.D. Rogers, *Organometallics* 4 (1985) 1485.
- [13] S.J. Mason, C.H. Mill, V.J. Murphy, D. O'Hare, D.J. Watkin, *J. Organomet. Chem.* 485 (1995) 165.
- [14] (a) R.M. Churchill, K. Gold, C.E. Maw, *Inorg. Chem.* 9 (1970) 1587. (b) A. Hayashi, K. Nakajima, M. Nonoyama, *Polyhedron* 16 (1997) 4087.
- [15] Atomic radii: $r(\text{C}_{\text{sp}^2}) = 0.667$, $r(\text{N}_{\text{sp}^2}) = 0.62$ Å in: L. Pauling, *Die Natur der chemischen Bindung*, VCH, Weinheim, 1962.
- [16] P.R. Sharp, A.J. Bard, *Inorg. Chem.* 22 (1983) 2689.
- [17] S. Trofimenko, *J. Am. Chem. Soc.* 89 (1967) 3904.
- [18] (a) P.R. Branson, R.A. Cable, M. Green, M.K. Lloyd, *J. Chem. Soc., Dalton Trans.* (1976) 12. (b) P.R. Branson, R.A. Cable, M. Green, M.K. Lloyd, *J. Chem. Soc. Chem. Commun.* (1974) 364. (c) A. Nakamura, Y. Tatsuno, S. Otsuka, *Inorg. Chem.* 11 (1972) 2058. (d) J.A. McCleverty, J. Williams, *Trans. Met. Chem.* 3 (1978) 201. (e) J.A. McCleverty, J. Williams, *Trans. Met. Chem.* 1 (1976) 288. (f) J.A. McCleverty, J. Williams, *Inorg. Synth.* 3 (1966) 211.
- [19] W.P. Fehlhammer, M. Fritz, *Chem. Rev.* 93 (1993) 1243.
- [20] (a) R.J. Cross, in: E.W. Abel, F.G.A. Stone, G. Wilkinson (Eds.), *Comprehensive Organometallic Chemistry*, second edition, vol. 9, Pergamon, Oxford, 1995, pp. 419. (b) S. Roy, R.J. Puddephatt, J.D. Scott, *J. Chem. Soc., Dalton Trans.* (1989) 2121.
- [21] D.D. Perrin, W. Armarego, D.R. Perrin, *Purification of Laboratory Chemicals*, Pergamon, New York, 1985.
- [22] G. Jacob, C. Moinet, *Bull. Soc. Chim. Fr.* (1983) I-291.
- [23] G.M. Sheldrick, SHELX-97, Programs for Crystal Structure Solution, Universität Göttingen, Germany, 1997.
- [24] G. Germain, P. Main, M.M. Woolfsen, *Acta Crystallogr. Sect. A* 27 (1971) 368.
- [25] J.J. Stewart, Programme System for X-ray Crystallography, Computer Science Center, University of Maryland, USA, 1976.